

Theory of Epitaxial Growth of Borophene on Layered Electride: Thermodynamic Stability and Kinetic Pathway

Xiaojuan Ni, Huaqing Huang, Kyung-Hwan Jin, Zhengfei Wang, and Feng Liu*

Cite This: *J. Phys. Chem. C* 2020, 124, 6063–6069

Read Online

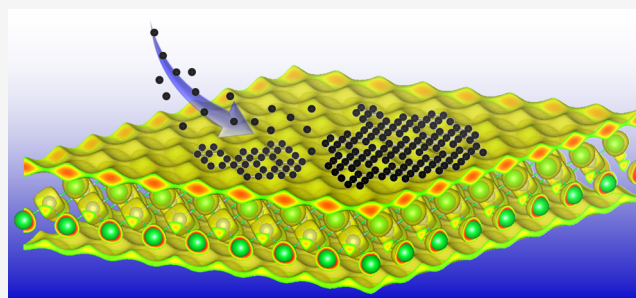
ACCESS |

Metrics & More

Article Recommendations

Supporting Information

ABSTRACT: Based on first-principles calculations, we propose that the layered electride can serve as an effective substrate, in place of a metal substrate, to grow borophene. We first confirm the thermodynamic stability of B@Sr₂N heterostructures by energetics analysis. Then, kinetically, we identify the atomistic pathways for a preferred 2D growth mode with a mixed triangle–hexagon configuration over 3D growth on the surface of Sr₂N, indicating the feasibility of epitaxial growth of borophene on layered electrides. As a weak metal, the significantly reduced density of states from the electride at the Fermi level helps to retain the most intrinsic electronic and transport properties of borophene, a significant advantage over the metal substrate. We envision that layered electrides provide an attractive family of substrates for epitaxial growth of a range of 2D materials that can otherwise only be grown on undesirable metal substrates.



INTRODUCTION

Two-dimensional (2D) materials have drawn intensive attention for both fundamental interests and potential applications.^{1–4} While high-quality small-size 2D materials, such as graphene^{5,6} and transition-metal dichalcogenides,^{7,8} may be prepared by mechanical exfoliation, it is highly desirable to grow 2D materials for large size and mass quantity to further our study and realize their potential applications. However, many 2D materials can only be grown on metal substrates, which is unwanted because the ample metallic states will inevitably destroy the intrinsic, especially nonmetallic properties of 2D materials. In this study, using borophene (a monolayer boron sheet) as a prototypical example, we demonstrate that layered electrides provide a new class of substrates, in place of metal, to effectively grow 2D materials with significant advantages.

Boron is one of the most versatile elements, forming various 3D bulk polymorphs.^{9–13} Similarly, different 2D borophene have been theoretically proposed^{14–20} and experimentally realized.^{21–25} In the well-known high-*T_c* superconductor MgB₂, boron possesses a planar honeycomb lattice, which is primarily responsible for the superconductivity.^{26,27} A recent study also showed MgB₂ to be a topological semimetal.²⁸ Besides honeycomb borophene, other borophene with mixed hexagonal–triangular geometry have also been theoretically predicted to superconduct.¹⁷ Thus, the synthesis of borophene may provide new opportunities for not only 2D high-*T_c* superconductivity but also topological superconductivity. However, the growth of borophene on a metal substrate has some drawbacks. It is unlikely to exfoliate the thin film of B@substrate away from the thick metal substrate. The high

conductivity of metal will mask the intrinsic transport properties of borophene due to the high electron density of states of metal near the Fermi level.²⁹ Therefore, searching for an insulating or weak metal substrate to grow borophene is of great interest.

Since boron has three valence electrons, the electron deficiency makes its structure energetically unstable. Thus, neither semiconductors nor insulators can serve as good substrates to grow borophene. Instead, we have identified layered electride, a “weak metal”, to be an effective substrate to grow borophene. Electrides are crystals with cavity-trapped electrons acting as anions.^{30–36} The concept of anionic electrons was first validated in alkali metal dissolved ammonia.^{37,38} Interestingly, a layered electride, dicalcium nitride (Ca₂N), was experimentally reported in 2013 to possess delocalized “2D electron gas (2DEG)” sandwiched between the cationic layers.³⁹ Ca₂N was then studied as an efficient electron donor for hydrogenation in alkynes and alkenes,⁴⁰ and the stability of honeycomb borophene in a sandwich geometry.⁴¹ Several carbides,^{42–46} nitrides,^{42,44–48} and oxides^{42,43,46} have since been predicted as layered electrides. We hypothesize that the presence of 2DEG on the layered electride surface provides an effective means to

Received: November 6, 2019

Revised: February 28, 2020

Published: March 2, 2020

compensate for the electron deficiency of borophene. In addition, the layered structure of electride can facilitate the exfoliation or growth of borophene on monolayer or thin films of electrides to minimize the substrate influence. Finally, as a weak metal, the significantly reduced density of states from the electride at the Fermi level helps to retain the most, if not all, of the intrinsic electronic and transport properties of borophene.

To test the above hypotheses, we investigate both the thermodynamic stability of B@Sr₂N and the kinetic pathways of boron growth on the Sr₂N surface using first-principles calculations. The choice of using layered electride Sr₂N as the prototypical substrate to grow borophene is because Sr₂N has been experimentally synthesized^{49,50} and has an appropriate lattice constant matched with borophene. We identify the atomistic kinetic pathways for boron growth on the Sr₂N surface with a preferred 2D growth mode over 3D mode. At large cluster size (~18 atoms), a mixed hexagonal and triangular geometry is favorable. All these findings point to the feasibility of the epitaxial growth of borophene on a layered electride.

COMPUTATIONAL METHODS

The first-principles calculations were performed using the Vienna ab initio simulation package (VASP) based on the projected augmented wave approach within the framework of density functional theory.^{51,52} The generalized gradient approximation in the Perdew, Burke, and Ernzerhof form (GGA-PBE) was used for the exchange–correlation functional.^{53,54} The cutoff energy of plane-wave basis was set to 500 eV. A vacuum layer with a thickness larger than 15 Å was adopted to study the 2D systems under the periodic boundary condition. The Brillouin zone integration was densely sampled according to the size of the supercell, ensuring approximately the same *k* point density for different sized structures. All the geometry structures were fully relaxed until the atomic force was less than 0.01 eV/Å.

RESULTS AND DISCUSSION

Bulk Sr₂N has a *R* $\bar{3}m$ space group with a lattice constant of 3.869 Å, and Figure 1a depicts the crystal structures of Sr₂N, similar to that of Ca₂N³⁹ and Y₂C.^{55,56} The building block of

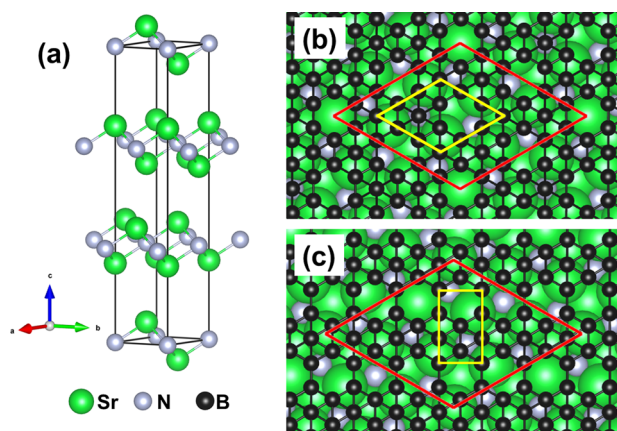


Figure 1. Crystal structures of (a) Sr₂N, (b) α -B@Sr₂N, and (c) β -B@Sr₂N. Red rhombus indicates the unit cell in the heterostructure. Yellow rhombus and rectangle indicate the unit cell in α - and β -borophene.

Sr₂N consists of three layers, where N atoms are sandwiched between two Sr layers. The calculated electron localization function (ELF) indicates the existence of interlayer free electrons in Sr₂N, as shown in Figure S1 in the Supporting Information (SI). Two borophene structures, α and β phases, as shown in Figure 1b,c are adopted to investigate the thermodynamic stability of the B@Sr₂N heterostructures, since α phase with $\eta = 1/9$ has been predicted to be a stable freestanding sheet⁵⁷ and β phase with $\eta = 1/6$ has been experimentally synthesized.²² Here, η is the density of hexagonal holes, which is defined as the ratio of the number of hexagonal holes to the number of atomic sites in the compact triangular borophene within a unit cell. Detailed structural information of B@Sr₂N is shown in Table S1 in the SI.

The substrate used to grow borophene plays a crucial role in stabilizing the structure. To better understand the stabilization mechanism, we calculate the formation energy of borophene on different substrates and perform the Bader charge analysis.⁵⁸ The formation energy is defined as

$$E_f = \frac{E_{\text{tot}} - E_{\text{sub}} - N \times E_B}{N} \quad (1)$$

where E_{tot} is the total energy of borophene on the substrate, E_{sub} is the energy of the substrate, E_B is the energy of the isolated boron atom, and N is the number of boron atoms.⁵⁹ A negative value of E_f means that the growth is a favorable process with respect to the clean surface and an isolated B atom. We take the energy of isolated boron atom as E_B in addition to the cohesive energy of bulk α -B₁₂ (as used in the previous calculations^{23,60}) because atomic boron source prepared by e-beam evaporator under ultrahigh vacuum condition is used during growth.^{21–23} The calculated formation energy and average charge transfer in B@Sr₂N and B@Ag(111) (see Table S1 and Figure S2 in the SI for structures) are listed in Table 1. As a comparison, we calculate

Table 1. Formation Energy in Reference to the Energy of Isolated Boron Atom and Averaged Charge Transfer in B@Sr₂N and B@Ag(111)^a

heterostructure	E_f (eV/atom)	charge transfer (e/atom)
α -B@Sr ₂ N	−6.322 (0.164)	0.106
β -B@Sr ₂ N	−6.348 (0.138)	0.107
α -B@Ag(111)	−6.131 (0.356)	0.025
β -B@Ag(111)	−6.173 (0.314)	0.039

^aThe formation energy in parentheses is calculated using the cohesive energy of bulk α -B₁₂ as the reference of boron atom.

the formation energy in reference to the cohesive energy of bulk α -B₁₂ as E_B , as shown in Table 1. Apparently, there is no significant difference in the formation energy and electron transfer between B@Sr₂N and B@Ag(111), which indicates that the layered electride Sr₂N could potentially replace conventional metal substrates to grow borophene.

We also study the distribution of onsite charge transfer of boron atoms in heterostructures from Bader charge analysis, as shown in Figure 2. A common feature is that most of the 6-coordinated boron atoms act as electron donors, and extra electrons are predominantly situated on 4- or 5-coordinated boron atoms surrounding the hexagonal holes, which act as electron acceptors. Therefore, the density of hexagonal holes may eventually reach the maximum, which is 1/3 in

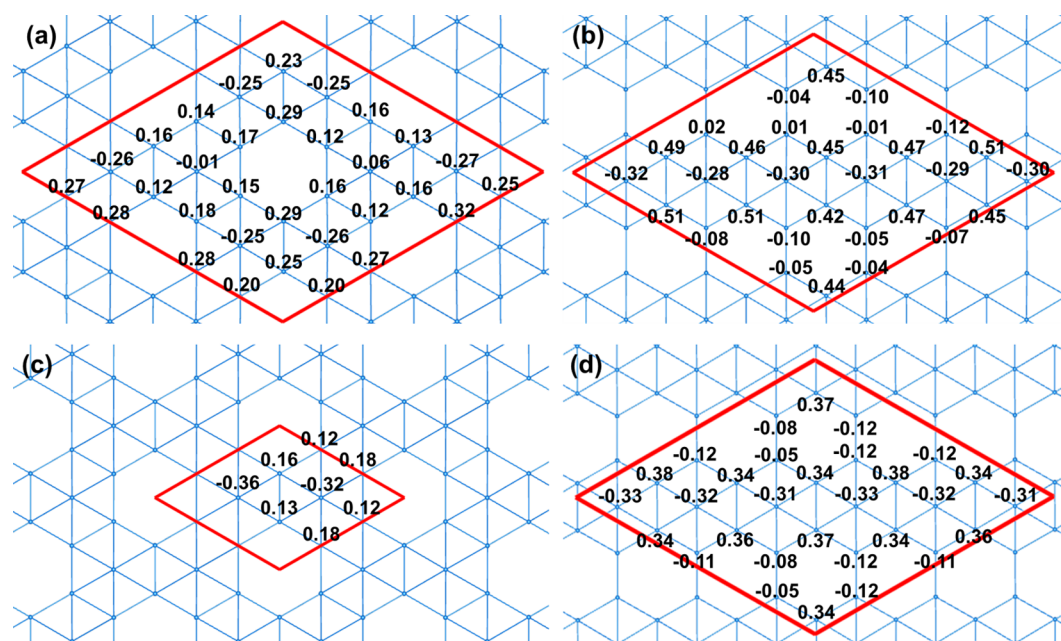


Figure 2. Distribution of onsite charge transfer from Bader charge analysis for (a) α -B@Sr₂N, (b) β -B@Sr₂N, (c) α -B@Ag(111), and (d) β -B@Ag(111). Positive (negative) value represents electron accumulation (depletion). Red rhombus indicates the unit cell. To more clearly show the charge distribution, only the boron lattice is presented without the Sr₂N substrate.

honeycomb structure if sufficient electrons are transferred to boron.

Next, we establish the preferred growth mode and identify the atomic pathways for boron growth on the Sr₂N substrate by investigating the initial stage of growth up to 18 atoms. Although the growth of borophene on metal substrates^{60–64} has been studied previously, fundamental mechanisms of borophene growth on layered electride are unknown. We adopted a 5 × 5 monolayer Sr₂N as the substrate, which is confirmed to be sufficiently large to avoid the intercluster interaction for up to 36-atom clusters, as shown in Figure 3. For the 36-atom boron cluster on the Sr₂N surface (Figure 3a), we calculated the corresponding ELF, as shown in Figure 3b. The contour plots of cuts 1 and 2 in ELF shown in Figure 3c,d

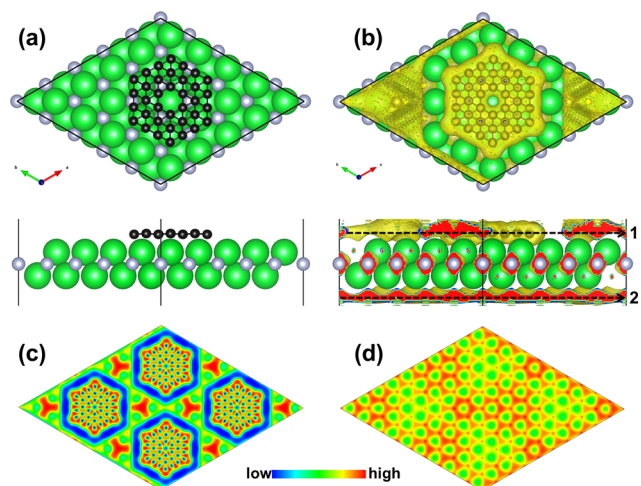


Figure 3. (a) Top and side views of a boron cluster ($N = 36$) on 5 × 5 Sr₂N surface. (b) Top and side views of ELF for (a). (c, d) Contour plots of ELF for a 2 × 2 supercell along the cuts 1 and 2 as indicated in (b).

explicitly indicate that the 5 × 5 supercell of Sr₂N is large enough to avoid the interaction from the neighboring boron clusters for the size of $N \leq 36$.

We first determine the preferred adsorption site for boron adatom. Figure 4 shows the nudged elastic band (NEB)

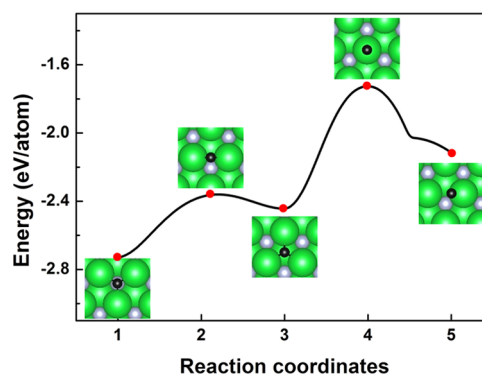


Figure 4. NEB calculation for boron atom diffusion on the Sr₂N surface. The insets present the adsorption structures at the local minima and saddle points, indicated by red dots.

calculation for boron atom diffusion on the Sr₂N surface. The insets present the adsorption structures at the local minima and saddle points, labeled as 1–5. The most stable is site 1 (top of middle N atom), followed by site 3 (top of bottom Sr atom). The other two positions are saddle points, such as site 2 (center of bridge_{1–3}) and site 4 (above top Sr atom). Site 5 is the local minima but has higher energy than sites 1 and 3. Hence, we tend to use sites 1 and 3 to construct the geometries for boron clusters at the initial stage of growth.

After structural relaxation, the preferred stable configurations of small boron clusters ($N = 2–10$) are depicted in Figure 5a–i, respectively. As illustrated in Figure 5a, the most stable positions for a boron dimer are sites 1 and 3, which is expected from the adatom adsorption energy. For a larger

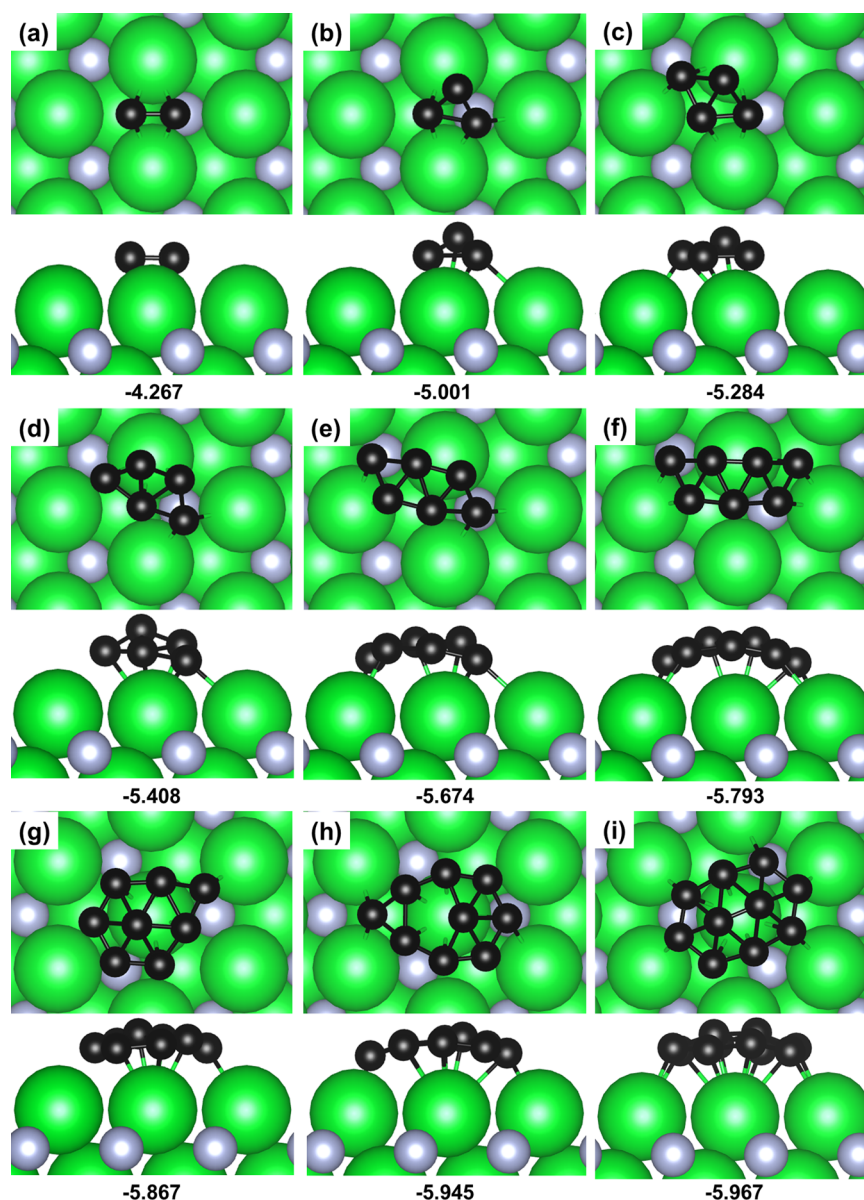


Figure 5. Top and side views of the preferred 2D configurations of boron clusters on the Sr_2N surface: (a) dimer, (b) trimer, (c) tetramer, (d) pentamer, (e) hexamer, (f) heptamer, (g) octamer, (h) nonamer, and (i) decamer. The numbers indicate the formation energy in the unit of eV/atom.

cluster, such as a trimer, a triangular structure occupying sites 1 and 3 is most stable, as shown in Figure 5b. Adding another adatom to the triangle trimer, it prefers to diffuse to the periphery to form a 2D rhomboid-shaped tetramer (Figure 5c), with two atoms located in site 1 and one located in site 3. By continuously adding adatom, the pentamer (Figure 5d), hexamer (Figure 5e), and heptamer (Figure 5f) are formed in sequence, and they all have the 2D structures as the most stable configurations. The hexamer with a hexagonal 6-ring geometry will transform into a rhomboid, which is the same as that in Figure 5e. For octamer and decamer, the compact-triangular structures (Figure 5g,i) are most stable, and for nonamer, the network with one pentagon is the most stable configuration (Figure 5h). In particular, all the preferred 2D configurations have the adatoms mostly occupying exclusively sites 1 and 3, and buckled 3D clusters are less stable than the corresponding 2D ones (see Figure S3 in the SI for details). In addition, we also performed the NEB calculations of boron

atom diffusing from the periphery to the top of the 2D cluster, and there is a diffusion barrier of ~ 0.55 eV/atom to form a 3D cluster (see Figure S4 in the SI).

Due to the numerous possible geometries for large boron clusters, we cannot exhaust all of them through calculations. Therefore, we use six boron clusters with $N = 18$ as a typical example to illustrate the relative stability of boron clusters between mixed triangle–hexagon and compact-triangular configurations. As shown in Figure 6, clusters with hexagonal hole (Figure 6a–c) are more stable than the compact structures (Figure 6d–f). The most stable boron cluster in Figure 6a has a triangular geometry with a hexagonal hole in the center, which is the signature structural motif in α -borophene. Another two clusters, the triangle-belt structure in Figure 6b with a hexagonal hole in the middle and the triangle-based geometry with a hexagonal hole on the periphery in Figure 6c, are metastable with the formation energy of 0.094 and 0.097 eV/atom higher than that of the stable one,

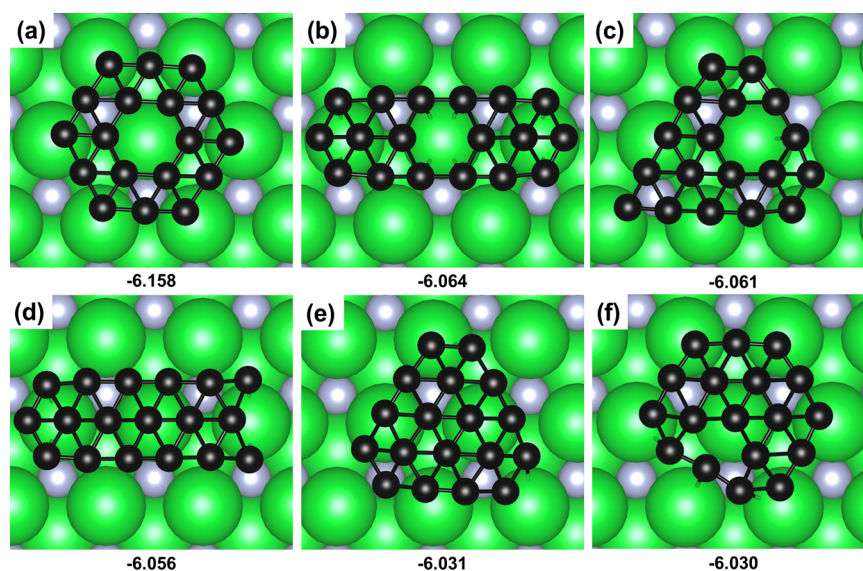


Figure 6. 2D configurations of boron clusters ($N = 18$) on the Sr_2N surface. The numbers indicate the formation energy in the unit of eV/atom.

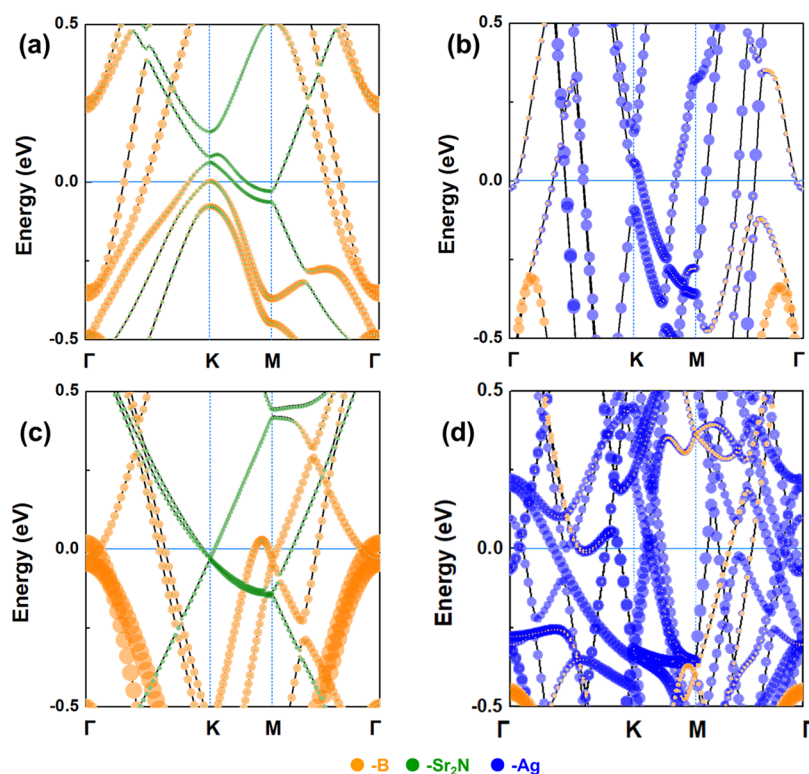


Figure 7. Band structures of (a) $\alpha\text{-B@Sr}_2\text{N}$, (b) $\alpha\text{-B@Ag}(111)$, (c) $\beta\text{-B@Sr}_2\text{N}$, and (d) $\beta\text{-B@Ag}(111)$. The orange, green, and blue indicate the contribution from B, Sr_2N , and Ag, respectively.

respectively. Therefore, the triangle and hexagon mixed boron clusters are more stable than compact-triangular ones on the surface of Sr_2N . We further confirmed this at the infinite 2D limit of a periodic structure. We constructed the configurations of borophene with different densities of hexagonal holes $\eta = 0, 1/36, 1/18, 1/12,$ and $1/3$ (Figure S5 in the SI) and calculated their formation energies, which are less stable than $\alpha\text{-}$ and $\beta\text{-B@Sr}_2\text{N}$ owing to the excessive electrons in compact-triangular borophene ($\eta = 0$) and the deficient electrons in honeycomb structure ($\eta = 1/3$), respectively. The above results imply that the electride substrate facilitates not only the 2D growth mode

of the planar island but also a transition to the ultimate triangle and hexagon mixed borophene sheet with the increasing coverage of boron atoms during growth.

Finally, after establishing the 2D growth of borophene on the Sr_2N substrate, we further briefly illustrate the advantage of the layered electride substrates over the conventional metal substrates. The calculated cleavage energy for $\alpha\text{-B@Ag}(111)$ is 1.47 J/m^2 , which is more than twice of 0.70 J/m^2 for $\alpha\text{-B@Sr}_2\text{N}$ (see Figure S6 in the SI). Therefore, the exfoliation of borophene with a thinner substrate from electride is much easier than that from metal. Specifically, two substrates made

of a monolayer Sr_2N versus a four-layer $\text{Ag}(111)$ for growing borophene are compared. The band structures of $\alpha\text{-B@Sr}_2\text{N}$, $\alpha\text{-B@Ag}(111)$, $\beta\text{-B@Sr}_2\text{N}$, and $\beta\text{-B@Ag}(111)$ are shown in Figure 7a–d, respectively. The orange, green, and blue indicate the contribution from B, Sr_2N , and Ag, respectively. One clearly sees that the electronic states of boron sheet in $\alpha\text{-B@Sr}_2\text{N}$ and $\beta\text{-B@Sr}_2\text{N}$ are much less perturbed than those in $\alpha\text{-B@Ag}(111)$ and $\beta\text{-B@Ag}(111)$ by the substrate because there are much less metallic states coming from the substrate. Bands of boron sheet in $\text{B@Sr}_2\text{N}$ are well-distinguished from those of Sr_2N , and, in contrast, boron bands in $\text{B@Ag}(111)$ are completely suppressed by those of Ag. In fact, the number of metallic states is severely underestimated using only four layers of Ag for $\alpha\text{-B@Ag}(111)$ and $\beta\text{-B@Ag}(111)$. This signifies a distinctive advantage of layered electride substrate over the metal substrate for growing borophene.

CONCLUSIONS

We propose for the first time that a layered electride can serve as an effective substrate to grow borophene. Both thermodynamic stability of $\text{B@Sr}_2\text{N}$ and kinetic pathways of boron growth have been investigated using first-principles calculations. The free electrons in the Sr_2N surface will compensate for the electron deficiency in borophene to stabilize the structure and facilitate the 2D growth mode. Our findings open a new avenue for epitaxial growth of borophene using layered electride substrates with notable advantages over metal substrates, which will stimulate immediate theoretical and experimental interests. Broadly speaking, the layered electrides may be used as effective substrates for epitaxial growth of various 2D materials that can otherwise only be grown on undesirable metal substrates.

ASSOCIATED CONTENT

Supporting Information

The Supporting Information is available free of charge at <https://pubs.acs.org/doi/10.1021/acs.jpcc.9b10438>.

ELF of bulk Sr_2N ; NEB calculation for boron atom diffusion between 2D and 3D clusters; energy of $\text{B@Sr}_2\text{N}$ as a function of density of hexagonal holes (PDF)

AUTHOR INFORMATION

Corresponding Author

Feng Liu – Department of Materials Science and Engineering, University of Utah, Salt Lake City, Utah 84112, United States; orcid.org/0000-0002-3701-8058; Email: fliu@eng.utah.edu

Authors

Xiaojuan Ni – Department of Materials Science and Engineering, University of Utah, Salt Lake City, Utah 84112, United States; orcid.org/0000-0002-5845-7404

Huaqing Huang – Department of Materials Science and Engineering, University of Utah, Salt Lake City, Utah 84112, United States; orcid.org/0000-0002-0283-8603

Kyung-Hwan Jin – Department of Materials Science and Engineering, University of Utah, Salt Lake City, Utah 84112, United States; orcid.org/0000-0002-5116-9987

Zhengfei Wang – Hefei National Laboratory for Physical Sciences at the Microscale, CAS Key Laboratory of Strongly-Coupled Quantum Matter Physics, University of Science and

Technology of China, Hefei, Anhui 230026, China; orcid.org/0000-0002-0788-9725

Complete contact information is available at:

<https://pubs.acs.org/10.1021/acs.jpcc.9b10438>

Notes

The authors declare no competing financial interest.

ACKNOWLEDGMENTS

This work is supported by U.S. Department of Energy-Basic Energy Sciences (Grant No. DE-FG02-04ER46148). We acknowledge DOE-NERSC and CHPC at the University of Utah for providing the computing resources.

REFERENCES

- (1) Geim, A. K.; Novoselov, K. S. The Rise of Graphene. *Nat. Mater.* **2007**, *6*, 183–191.
- (2) Liu, Z.; Wang, Z. F.; Mei, J. W.; Wu, Y. S.; Liu, F. Flat Chern Band in a Two-Dimensional Organometallic Framework. *Phys. Rev. Lett.* **2013**, *110*, No. 106804.
- (3) Wang, Z. F.; Jin, K.; Liu, F. Computational Design of Two-Dimensional Topological Materials. *WIREs Comput. Mol. Sci.* **2017**, *7*, No. e1304.
- (4) Ni, X.; Jiang, W.; Huang, H.; Jin, K. H.; Liu, F. Intrinsic Quantum Anomalous Hall Effect in a Two-Dimensional Anilato-Based Lattice. *Nanoscale* **2018**, *10*, 11901–11906.
- (5) Novoselov, K. S.; Geim, A. K.; Morozov, S. V.; Jiang, D.; Zhang, Y.; Dubonos, S. V.; Grigorieva, I. V.; Firsov, A. A. Electric Field Effect in Atomically Thin Carbon Films. *Science* **2004**, *306*, 666–669.
- (6) Novoselov, K. S.; Geim, A. K.; Morozov, S. V.; Jiang, D.; Katsnelson, M. I.; Grigorieva, I. V.; Dubonos, S. V.; Firsov, A. A. Two-Dimensional Gas of Massless Dirac Fermions in Graphene. *Nature* **2005**, *438*, 197–200.
- (7) Novoselov, K. S.; Jiang, D.; Schedin, F.; Booth, T. J.; Khotkevich, V. V.; Morozov, S. V.; Geim, A. K. Two-Dimensional Atomic Crystals. *Proc. Natl. Acad. Sci. U.S.A.* **2005**, *102*, 10451–10453.
- (8) Wang, Q. H.; Kalantar-Zadeh, K.; Kis, A.; Coleman, J. N.; Strano, M. S. Electronics and Optoelectronics of Two-Dimensional Transition Metal Dichalcogenides. *Nat. Nanotechnol.* **2012**, *7*, 699–712.
- (9) Zhang, Z.; Penev, E. S.; Yakobson, B. I. Two-Dimensional Boron: Structures, Properties and Applications. *Chem. Soc. Rev.* **2017**, *46*, 6746–6763.
- (10) Albert, B.; Hillebrecht, H. Boron: Elementary Challenge for Experimenters and Theoreticians. *Angew. Chem., Int. Ed.* **2009**, *48*, 8640–8668.
- (11) Oganov, A. R.; Chen, J.; Gatti, C.; Ma, Y.; Ma, Y.; Glass, C. W.; Liu, Z.; Yu, T.; Kurakevych, O. O.; Solozhenko, V. L. Ionic High-Pressure Form of Elemental Boron. *Nature* **2009**, *457*, 863–867.
- (12) Ball, P. Material Witness: Why Is Boron so Hard? *Nat. Mater.* **2010**, *9*, 6.
- (13) Sands, D. E.; Hoard, J. L. Rhombohedral Elemental Boron. *J. Am. Chem. Soc.* **1957**, *79*, 5582–5583.
- (14) Zhang, L. Z.; Yan, Q. B.; Du, S. X.; Su, G.; Gao, H. J. Boron Sheet Adsorbed on Metal Surfaces: Structures and Electronic Properties. *J. Phys. Chem. C* **2012**, *116*, 18202–18206.
- (15) Zhang, Z.; Mannix, A. J.; Hu, Z.; Kiraly, B.; Guisinger, N. P.; Hersam, M. C.; Yakobson, B. I. Substrate-Induced Nanoscale Undulations of Borophene on Silver. *Nano Lett.* **2016**, *16*, 6622–6627.
- (16) Xu, S. G.; Li, X. T.; Zhao, Y. J.; Liao, J. H.; Xu, H.; Yang, X. B. An Electron Compensation Mechanism for the Polymorphism of Boron Monolayers. *Nanoscale* **2018**, *10*, 13410–13416.
- (17) Penev, E. S.; Kutana, A.; Yakobson, B. I. Can Two-Dimensional Boron Superconduct? *Nano Lett.* **2016**, *16*, 2522–2526.

- (18) Zhou, X. F.; Dong, X.; Oganov, A. R.; Zhu, Q.; Tian, Y.; Wang, H. T. Semimetallic Two-Dimensional Boron Allotrope with Massless Dirac Fermions. *Phys. Rev. Lett.* **2014**, *112*, No. 085502.
- (19) Zhang, Z.; Shirodkar, S. N.; Yang, Y.; Yakobson, B. I. Gate-Voltage Control of Borophene Structure Formation. *Angew. Chem., Int. Ed.* **2017**, *56*, 15421–15426.
- (20) Penev, E. S.; Bhowmick, S.; Sadrzadeh, A.; Yakobson, B. I. Polymorphism of Two-Dimensional Boron. *Nano Lett.* **2012**, *12*, 2441–2445.
- (21) Mannix, A. J.; Zhou, X.-F.; Kiraly, B.; Wood, J. D.; Alducin, D.; Myers, B. D.; Liu, X.; Fisher, B. L.; Santiago, U.; Guest, J. R.; et al. Synthesis of Borophenes: Anisotropic, Two-Dimensional Boron Polymorphs. *Science* **2015**, *350*, 1513–1516.
- (22) Feng, B.; Zhang, J.; Zhong, Q.; Li, W.; Li, S.; Li, H.; Cheng, P.; Meng, S.; Chen, L.; Wu, K. Experimental Realization of Two-Dimensional Boron Sheets. *Nat. Chem.* **2016**, *8*, 563–568.
- (23) Li, W.; Kong, L.; Chen, C.; Gou, J.; Sheng, S.; Zhang, W.; Li, H.; Chen, L.; Cheng, P.; Wu, K. Experimental Realization of Honeycomb Borophene. *Sci. Bull.* **2018**, *63*, 282–286.
- (24) Wu, R.; Drozdov, I. K.; Eltinge, S.; Zahl, P.; Ismail-beigi, S.; Božović, I.; Gozar, A. Large-Area Single-Crystal Sheets of Borophene on Cu(111) Surfaces. *Nat. Nanotechnol.* **2019**, *14*, 44–49.
- (25) Wu, R.; Gozar, A.; Božović, I. Large-Area Borophene Sheets on Sacrificial Cu(111) Films Promoted by Recrystallization from Subsurface Boron. *npj Comput. Mater.* **2019**, *4*, No. 40.
- (26) Buzea, C.; Tsutomu, Y. Review of the Superconducting Properties of MgB₂. *Supercond. Sci. Technol.* **2001**, *14*, R115–R146.
- (27) An, J. M.; Pickett, W. E. Superconductivity of MgB₂: Covalent Bonds Driven Metallic. *Phys. Rev. Lett.* **2001**, *86*, 4366–4369.
- (28) Jin, K.; Huang, H.; Mei, J.-W.; Liu, Z.; Lim, L.-K.; Liu, F. Topological Superconducting Phase in High-*T_c* Superconductor MgB₂ with Dirac-Nodal-Line Fermions. *npj Comput. Mater.* **2019**, *5*, No. 57.
- (29) Levinson, H. J.; Greuter, F.; Plummer, E. W. Experimental Band Structure of Aluminum. *Phys. Rev. B* **1983**, *27*, 727–747.
- (30) Ellaboudy, A.; Dye, J. L.; Smith, P. B. Cesium 18-Crown-6 Compounds. A Crystalline Cesium and a Crystalline Electride. *J. Am. Chem. Soc.* **1983**, *105*, 6490–6491.
- (31) Toda, Y.; Matsuishi, S.; Hayashi, K.; Ueda, K.; Kamiya, T.; Hirano, M.; Hosono, H. Field Emission of Electron Anions Clathrated in Subnanometer-Sized Cages in [Ca₂₄Al₂₈O₆₄]⁴⁺(4e⁻). *Adv. Mater.* **2004**, *16*, 685–689.
- (32) Dye, J. L. Electrides: Early Examples of Quantum Confinement. *Acc. Chem. Res.* **2009**, *42*, 1564–1572.
- (33) Kim, S. W.; et al. Solvated Electrons in High-Temperature Melts and Glasses of the Room-Temperature Stable Electride [Ca₂₄Al₂₈O₆₄]⁴⁺(4e⁻). *Science* **2011**, *333*, 71–74.
- (34) Chanhom, P.; Fritz, K. E.; Burton, L. A.; Kloppenburg, J.; Filinchuk, Y.; Senyshyn, A.; Wang, M.; Feng, Z.; Insin, N.; Suntivich, J.; et al. Sr₃CrN₃: A New Electride with a Partially Filled d-Shell Transition Metal. *J. Am. Chem. Soc.* **2019**, *141*, 10595–10598.
- (35) Dale, S. G.; Johnson, E. R. Theoretical Descriptors of Electrides. *J. Phys. Chem. A* **2018**, *122*, 9371–9391.
- (36) Wang, J.; Sui, X.; Gao, S.; Duan, W.; Liu, F.; Huang, B. Anomalous Dirac Plasmons in 1D Topological Electrides. *Phys. Rev. Lett.* **2019**, *123*, No. 206402.
- (37) Kraus, C. A. Solution of Metals in Non-Metallic Solvents; I. General Properties of Solutions of Metals in Liquid Ammonia. *J. Am. Chem. Soc.* **1907**, *29*, 1557–1571.
- (38) Kraus, C. A. Solutions of Metals in Non-Metallic Solvents; IV. Material Effects Accompanying the Passage of an Electrical Current through Solutions of Metals in Ammonia. Migration Experiments. *J. Am. Chem. Soc.* **1908**, *30*, 1323–1344.
- (39) Lee, K.; Kim, S. W.; Toda, Y.; Matsuishi, S.; Hosono, H. Dicalcium Nitride as a Two-Dimensional Electride with an Anionic Electron Layer. *Nature* **2013**, *494*, 336–340.
- (40) Kim, Y. J.; Kim, S. M.; Cho, E. J.; Hosono, H.; Yang, J. W.; Kim, S. W. Two Dimensional Inorganic Electride-Promoted Electron Transfer Efficiency in Transfer Hydrogenation of Alkynes and Alkenes. *Chem. Sci.* **2015**, *6*, 3577–3581.
- (41) Liu, D.; Tománek, D. Effect of Net Charge on the Relative Stability of 2D Boron Allotropes. *Nano Lett.* **2019**, *19*, 1359–1365.
- (42) Tada, T.; Takemoto, S.; Matsuishi, S.; Hosono, H. High-Throughput Ab Initio Screening for Two-Dimensional Electride Materials. *Inorg. Chem.* **2014**, *53*, 10347–10358.
- (43) Ge, Y.; Guan, S.; Liu, Y. Two Dimensional Superconductors in Electrides. *New J. Phys.* **2012**, *19*, No. 123020.
- (44) Druffel, D. L.; Woomey, A. H.; Kuntz, K. L.; Pawlik, J. T.; Warren, S. C. Electrons on the Surface of 2D Materials: From Layered Electrides to 2D Electrenes. *J. Mater. Chem. C* **2017**, *5*, 11196–11213.
- (45) Inoshita, T.; Jeong, S.; Hamada, N.; Hosono, H. Exploration for Two-Dimensional Electrides via Database Screening and Ab Initio Calculation. *Phys. Rev. X* **2014**, *4*, No. 031023.
- (46) Zhang, Y.; Wang, H.; Wang, Y.; Zhang, L.; Ma, Y. Computer-Assisted Inverse Design of Inorganic Electrides. *Phys. Rev. X* **2017**, *7*, No. 011017.
- (47) Ming, W.; Yoon, M.; Du, M. H.; Lee, K.; Kim, S. W. First-Principles Prediction of Thermodynamically Stable Two-Dimensional Electrides. *J. Am. Chem. Soc.* **2016**, *138*, 15336–15344.
- (48) Tada, T.; Wang, J.; Hosono, H. First Principles Evolutionary Search for New Electrides along the Dimensionality of Anionic Electrons. *J. Comput. Chem., Jpn.* **2017**, *16*, 135.
- (49) Brese, N.; O’Keeffe, M. Synthesis, Crystal Structure, and Physical Properties of Sr₂N. *J. Solid State Chem.* **1990**, *87*, 134–140.
- (50) Inumaru, K.; Kuroda, Y.; Sakamoto, K.; Murashima, M.; Yamanaka, S. Synthesis and High Metallic Conductivity of Layer-Structured Sr₂N Thin Film Deposited onto MgO(001) Substrate. *J. Alloys Compd.* **2004**, *372*, L1–L3.
- (51) Kresse, G.; Hafner, J. Ab Initio Molecular Dynamics for Liquid Metals. *Phys. Rev. B* **1993**, *47*, 558–561.
- (52) Kresse, G.; Furthmüller, J. Efficient Iterative Schemes for Ab Initio Total-Energy Calculations Using a Plane-Wave Basis Set. *Phys. Rev. B* **1996**, *54*, 11169–11186.
- (53) Perdew, J. P.; Burke, K.; Ernzerhof, M. Generalized Gradient Approximation Made Simple. *Phys. Rev. Lett.* **1997**, *78*, 1396.
- (54) Perdew, J. P.; Burke, K.; Ernzerhof, M. Generalized Gradient Approximation Made Simple. *Phys. Rev. Lett.* **1996**, *77*, 3865–3868.
- (55) Zhang, X.; Xiao, Z.; Lei, H.; Toda, Y.; Matsuishi, S.; Kamiya, T.; Ueda, S.; Hosono, H. Two-Dimensional Transition-Metal Electride Y₂C. *Chem. Mater.* **2014**, *26*, 6638–6643.
- (56) Huang, H.; Jin, K. H.; Zhang, S.; Liu, F. Topological Electride Y₂C. *Nano Lett.* **2018**, *18*, 1972–1977.
- (57) Tang, H.; Ismail-Beigi, S. Novel Precursors for Boron Nanotubes: The Competition of Two-Center and Three-Center Bonding in Boron Sheets. *Phys. Rev. Lett.* **2007**, *99*, No. 115501.
- (58) Tang, W.; Sanville, E.; Henkelman, G. A Grid-Based Bader Analysis Algorithm without Lattice Bias. *J. Phys.: Condens. Matter* **2009**, *21*, No. 084204.
- (59) Donohue, J. *The Structures of the Elements*; Wiley: New York, 1974.
- (60) Liu, H.; Gao, J.; Zhao, J. From Boron Cluster to Two-Dimensional Boron Sheet on Cu(111) Surface: Growth Mechanism and Hole Formation. *Sci. Rep.* **2013**, *3*, No. 3238.
- (61) Boustani, I. Systematic Ab Initio Investigation of Bare Boron Clusters: Determination of the Geometry and Electronic Structures of B_n (N = 2–14). *Phys. Rev. B* **1997**, *55*, 16426–16438.
- (62) Liu, Y.; Penev, E. S.; Yakobson, B. I. Probing the Synthesis of Two-Dimensional Boron by First-Principles Computations. *Angew. Chem., Int. Ed.* **2013**, *125*, 3238–3241.
- (63) Zhang, Z.; Mannix, A. J.; Liu, X.; Hu, Z.; Guisinger, N. P.; Hersam, M. C.; Yakobson, B. I. Near-Equilibrium Growth from Borophene Edges on Silver. *Sci. Adv.* **2019**, *5*, No. eaax0246.
- (64) Zhang, Z.; Yang, Y.; Gao, G.; Yakobson, B. I. Two-Dimensional Boron Monolayers Mediated by Metal Substrates. *Angew. Chem., Int. Ed.* **2015**, *54*, 13022–13026.